

Supporting Information

Cocrystal of codeine and cyclopentobarbital

Thomas Gelbrich ^{1,*}, Jascha Schinke ¹ and Ulrich J. Griesser ¹

¹ Institute of Pharmacy, University of Innsbruck, Innrain 52c, A-6020 Innsbruck, Austria

* Correspondence: thomas.gelbrich@uibk.ac.at

Contents

1. Molecular geometry	3
2. Powder X-ray diffraction	4
3. Differential Scanning Calorimetry (DSC).....	5
4. Hot-stage microscopy.....	6
5. FTIR Spectroscopy.....	8
6. Methods.....	9
6.1. Powder X-ray diffraction.....	9
6.2. FTIR Spectroscopy	9
6.3. Differential scanning calorimetry	9
7. References	10

1. Molecular geometry

Table S1. Torsion angle τ and the angle formed by the mean planes defined by the rings *A/B/C* and *D/E* in solid forms of codeine.

CSD code	Torsion angle τ [°]	Planar angle (<i>A/B/C</i>), (<i>D/E</i>) [°]	Compound	Ref.
CCDC 2278182	88.2	25.2	(I)·(II)	<i>This work</i>
CDNECR	86.0	178.7	(I)Cr(CO) ₃	[1]
CODHBH	89.9	178.8	(IH ⁺)Br ⁻ · 2(H ₂ O)	[2]
EZEWAK	89.3	-176.3	^a	[3]
OPOQAN	87.2	-128.3	(IH ⁺)Cl ⁻	[4]
QITZOK (molecule A)	89.4	-130.9	(IH ⁺)H ₃ PO ₄ ⁻ · 1.5(H ₂ O)	[5]
QITZOK (molecule B)	89.4	-169.3	^b	^b
QUBSEM (molecule A)	89.4	25.4	(IH ⁺)H ₂ PO ₄ ⁻ · 0.5(H ₂ O)	[6]
QUBSEM (molecule B)	88.7	36.2	^b	^b
ZZZRFQ01	90.0	178.2	(IH ⁺)Cl ⁻ · 2(H ₂ O)	[4]
ZZZTSE03	88.1	-168.7	(I)	[7]
ZZZTZQ02	89.1	168.0	(I) · H ₂ O	[4]

^a Catena-[tetrakis(μ -2,4,6-tris(pyridin-4-yl)-1,3,5-triazine)-dodecaiodo-hexa-zinc(II) sesquikis(3-methoxy-17-methyl-7,8-didehydro-4,5-epoxymorphinan-6-ol) cyclohexane unknown solvate].

^b As in previous row.

2. Powder X-ray diffraction

The PXRD pattern of the bulk material is consistent with the reported single crystal structure of (I)·(II) (Figure S1; bottom). An additional comparison with PXRD reference patterns of anhydrous codeine (I) and three polymorphs of cyclopentobarbital (II) confirms the absence of any of these phases from the product.

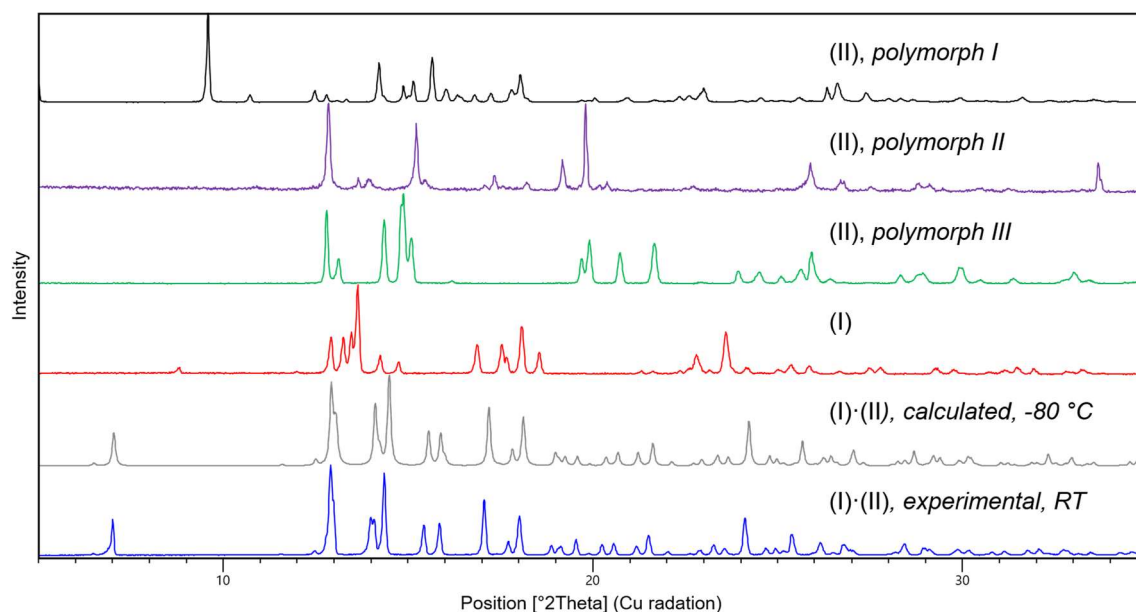


Figure S1. Powder X-ray diffractograms of polymorphs I (black), II (purple) and III (green) of cyclopentobarbital (I), codeine anhydrate (II) (red) and the cocrystal of codeine and cyclopentobarbital, (I)·(II) (grey: calculated from single crystal data at -80 °C; blue: experimental).

3. Differential Scanning Calorimetry (DSC)

Typical DSC traces of the cocrystal, the mother compounds and their physical mixture are shown in Figure S2. Thermoanalytical data of the cocrystal (I)·(II) are collected in Table S2. The cocrystal shows one sharp melting endotherm at 136.9 ± 0.3 °C (T_{onset} ; 95 % confidence interval) with a fusion enthalpy of 43.9 kJ mol⁻¹. No recrystallization of the cocrystal occurred on cooling of the melt.

The DSC trace for codeine anhydrate shows a melting at 156.6 °C (T_{onset}). Polymorph III of cyclopentobarbital displays incongruent melting behavior. The melting endotherm of polymorph III at 123.4 °C is followed by the crystallization and subsequent melting of polymorph I. The 1:1 physical mixture of (I) and (II) exhibits a single broad endothermic event between about 80 and 150 °C, which indicates eutectic melting without a crystallization of the cocrystal.

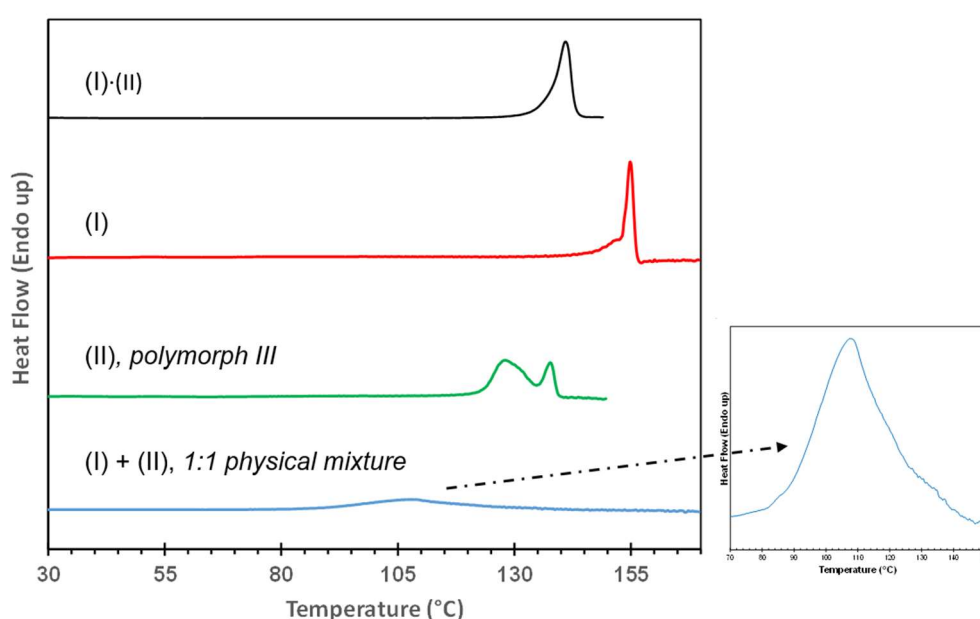


Fig. S2 DSC traces of the cocrystal (I)·(II), codeine anhydrate, cyclopentobarbital (polymorph III) and a 1:1 physical mixture of codeine and cyclopentobarbital; heating rate: 10 K min⁻¹.

Table S2. Thermoanalytical data of the cocrystal (I)·(II)

Parameter	Value
T_{fus} (°C) ^a	
DSC (onset)	136.9 ± 0.3
HSM (melting equilibrium)	140.1
$\Delta_{\text{fus}}H$ (kJ mol ⁻¹) ^b	43.9 ± 0.1
$\Delta_{\text{fus}}S$ (J mol ⁻¹ K ⁻¹) ^c	107.1 ± 0.2

^a Melting point.

^b Enthalpy of fusion.

^c Entropy of fusion; errors calculated as 95% confidence interval.

4. Hot-stage microscopy

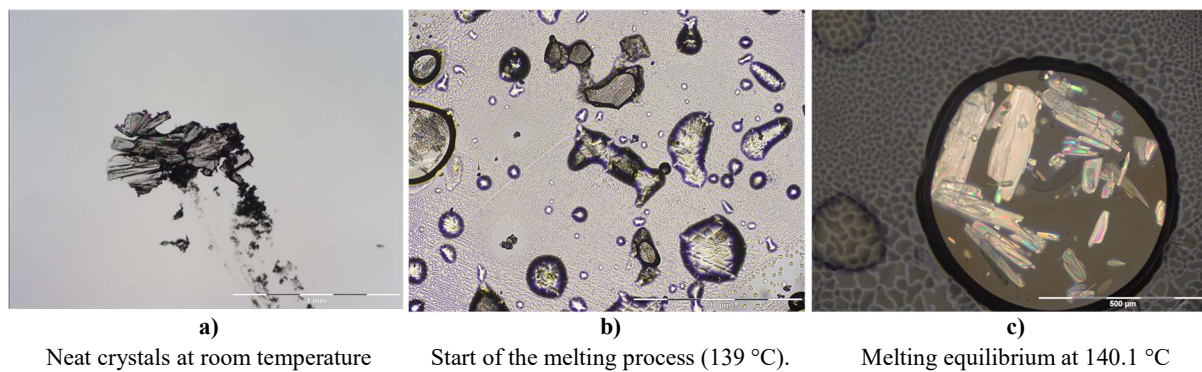


Figure S3. Photomicrographs of the cocrystal (I)·(II).

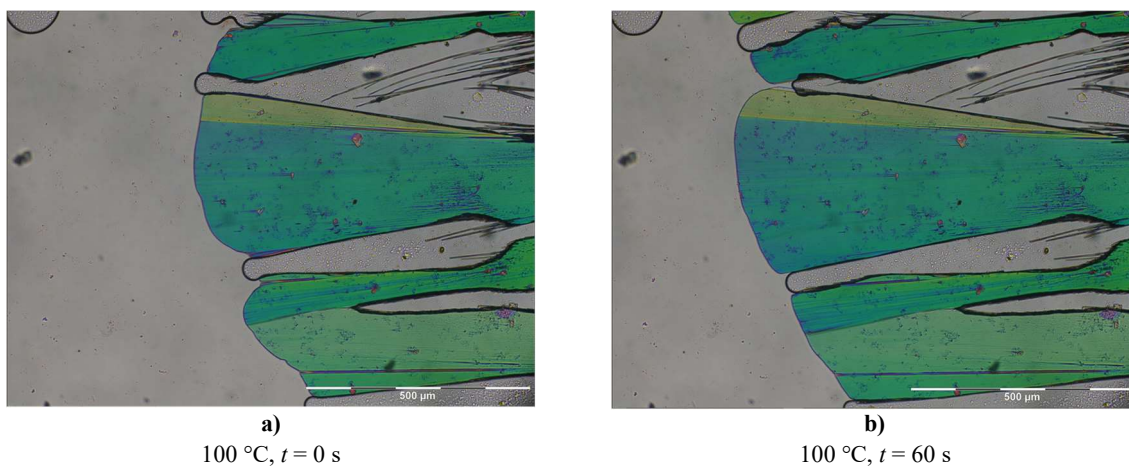


Figure S4. Microscopic film preparation showing the growth of the cocrystal (I)·(II) from the melt.

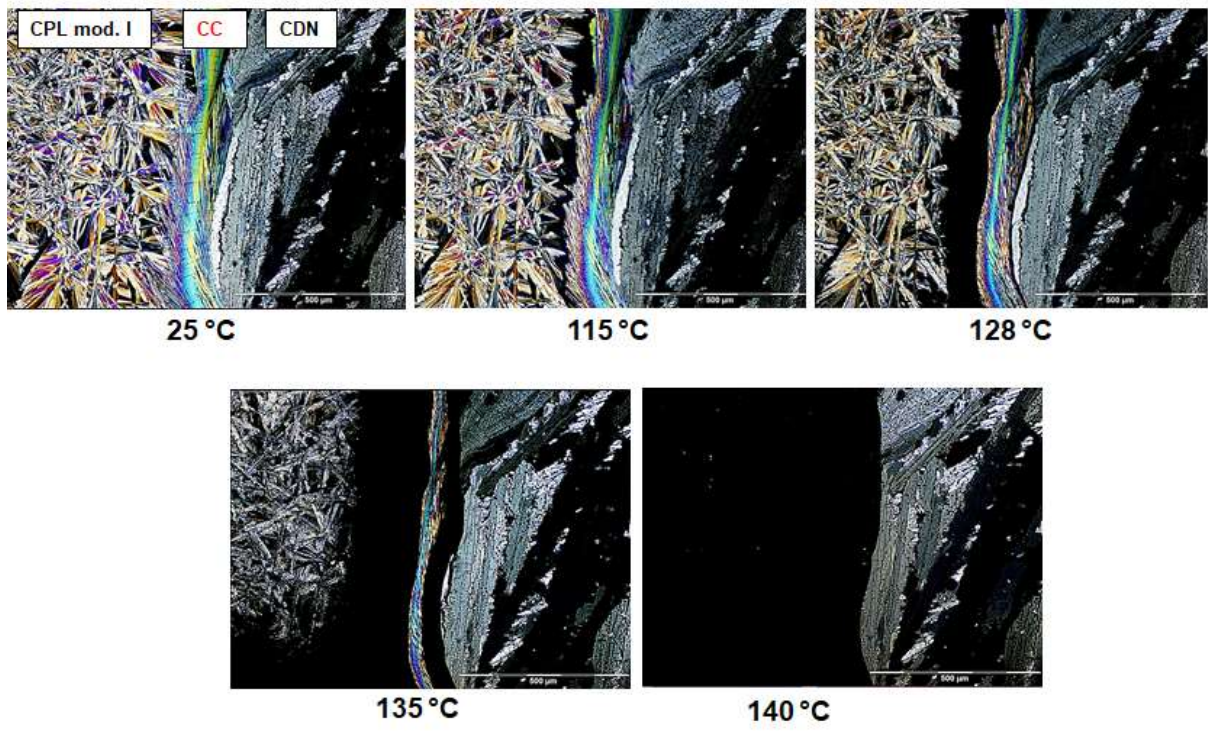


Figure S5. Polarized-light photomicrographs of a contact preparation of codeine (“CPL mod. I”) with cyclopentobarbital (“CDN”); “CC”: cocystal (I)-(II).

5. FTIR Spectroscopy

The FTIR spectrum of the cocrystal (Figure S6) shows a bathochromic shift of the OH stretching vibration from 3531 cm^{-1} to 3416 cm^{-1} in comparison to the spectrum of codeine. This implies a stronger hydrogen bond interaction in the cocrystal, which is consistent with the data of the single crystal structure. Polymorph III of cyclopentobarbital shows three NH vibrations between approximately 3320 and 3090 cm^{-1} , whereas the cocrystal exhibits only two peaks in this region. The observed C=O vibrations (1760 and 1670 cm^{-1}) are consistent with the presence of the barbiturate component in the cocrystal. Their shift in comparison to spectrum of cyclopentobarbital ($\nu\text{ C=O}$: 1756 , 1714 and 1675 cm^{-1}) is consistent with the observed alteration in hydrogen-bond interactions. The fact that most of the bands in the fingerprint region are shifted compared to the mother phases (including any polymorphs) is a further simple proof for the formation of a cocrystal, along with the absence of an absorption in the spectral range between 2700 and 2200 cm^{-1} which would indicate the formation of a salt ($\nu\text{ N}^+\text{-H}$).

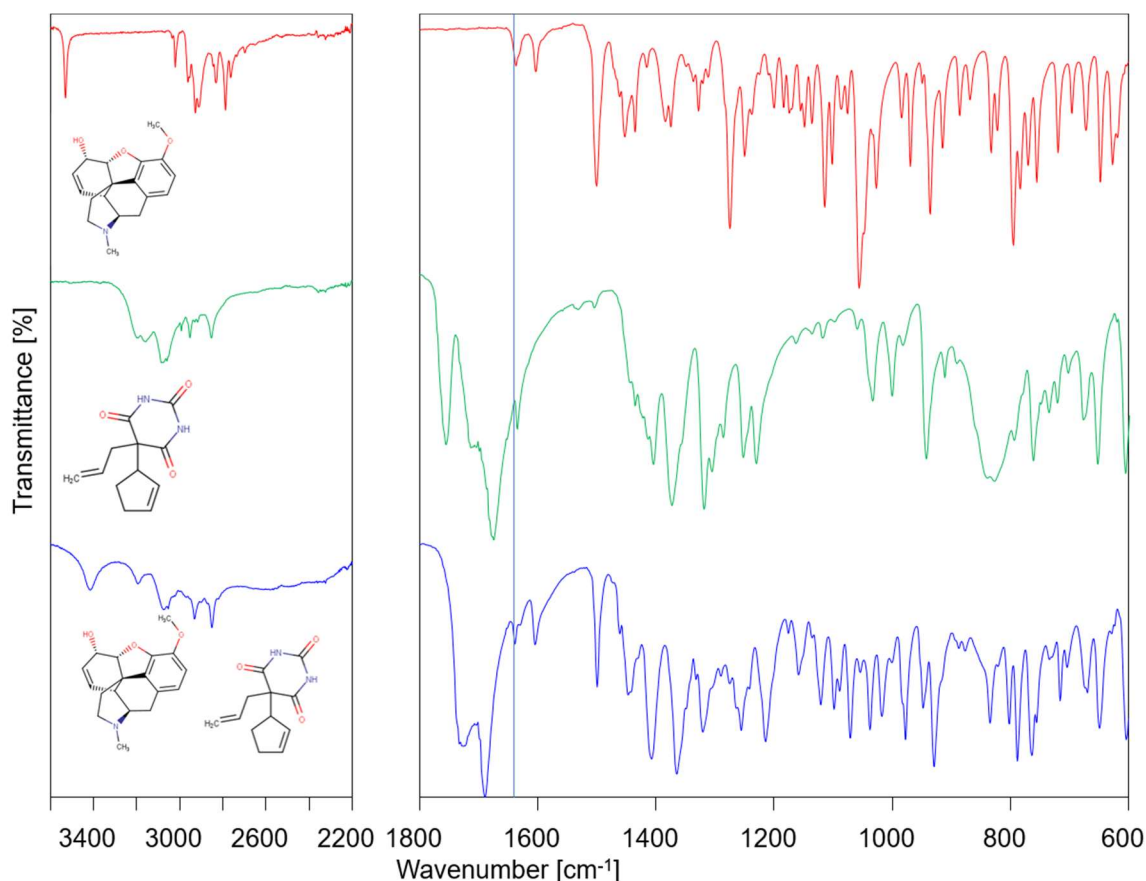


Figure S6. FTIR spectra of codeine anhydrate (I), polymorph III of cyclopentobarbital (II) and their 1:1 cocrystal (I)·(II).

6. Methods

6.1. Powder X-ray diffraction

The PXRD patterns were obtained with an X'Pert PRO diffractometer (PANalytical, Almelo, The Netherlands) equipped with a θ/θ coupled goniometer in transmission geometry, programmable XYZ stage with well plate holder, Cu-K $\alpha_{1,2}$ radiation source with a focusing mirror, a 0.5° divergence slit, a 0.02° Soller slit collimator and a 0.5° anti-scattering slit on the incident beam side, a 2 mm anti-scattering slit, a 0.02° Soller slit collimator, a Ni filter and a solid state PIXcel^{1D} detector. The patterns were recorded at a tube voltage of 40 kV, tube current of 40 mA, applying a step-size of 0.013° 2θ with 40 s per step in the angular range of 2° to 40°.

6.2. FTIR Spectroscopy

Infrared spectra were recorded with a diamond ATR unit (PIKE GladiATR, Madison, US) on a Bruker Vertex 70 FTIR spectrometer (Bruker Analytische Messtechnik GmbH, Germany). The spectra were recorded between 4000 and 400 cm⁻¹ at an instrument resolution of 2 cm⁻¹ (32 scans per spectrum).

6.3. Differential scanning calorimetry

Differential scanning calorimetry was performed with a DSC 7 (PerkinElmer, Norwalk, Ct., USA). Approximately 1 to 5 ± 0.0005 mg sample (using a UM3 ultramicrobalance, Mettler, Greifensee, Switzerland) were weighed into Al-Pans (30 μ L) and sealed with a cover. Dry nitrogen was used as the purge gas (purge: 20 mL min⁻¹). The instrument was calibrated for temperature with pure benzophenone (mp. 48.0 °C) and caffeine (236.2 °C), and the energy calibration was performed with indium (mp. 156.6 °C, heat of fusion 28.45 J g⁻¹). The errors on the stated temperatures (extrapolated onset temperatures) and enthalpy values were calculated at the 95% confidence interval and are based on at least three measurements.

7. References

1. Arzeno, H. B.; Barton, D. H. R.; Davies, S. G.; Lusinchi, X.; Meunier, B.; Pascard, C. Synthesis of 10(S)-methylocodeine and 10(S)-methylophine, *Nouv. J. Chim.* **1980**, *4*, 369–375.
2. Kartha, G.; Ahmed, F. R.; Barnes, W. H. Refinement of the crystal structure of codeine hydrobromide dihydrate, and establishment of the absolute configuration of the codeine molecule. *Acta Crystallogr.* **1962**, *15*, 326–333. doi:10.1107/S0365110X62000821
3. Rosenberger, L.; von Essen, C.; Khutia, A.; Kühn, C.; Georgi, K.; Hirsch, A. K. H.; Hartmann, R. W.; Badolo, L. Crystalline sponge affinity screening: A fast tool for soaking condition optimization without the need of X-ray diffraction analysis, *Eur. J. Pharm. Sci.* **2021**, *164*, 105884. doi:10.1016/j.ejps.2021.105884
4. Braun, D. E.; Gelbrich, T.; Kahlenberg, V.; Griesser, U. J. Insights into Hydrate Formation and Stability of Morphinanes from a Combination of Experimental and Computational Approaches, *Mol. Pharm.* **2014**, *11*, 3145–3163. doi:10.1021/mp500334z
5. Runčevski, T.; Petruševski, G.; Makreski, P.; Ugarkovic, S.; Dinnebier, R. E. On the hydrates of codeine phosphate: the remarkable influence of hydrogen bonding on the crystal size, *Chem. Commun.* **2014**, *50*, 6970–6972. doi:10.1039/C4CC01430H
6. Langes, C.; Gelbrich, T.; Griesser, U. J.; Kahlenberg V. Codeine dihydrogen phosphate hemihydrate, *Acta Crystallogr. C* **2009**, *65*, o419–o422. doi:10.1107/s0108270109027164
7. Scheins, S.; Messerschmidt, M.; Morgenroth, W.; Paulmann, C.; Luger, P. Electron Density Analyses of Opioids: A Comparative Study, *J. Phys. Chem. A* **2007**, *111*, 5499–5508. doi:10.1021/jp0709252